

Applied Microbiology and Biotechnology

Caleosin-assembled oil bodies as a potential delivery nanocarrier

--Manuscript Draft--

Manuscript Number:	AMAB-D-11-01454R1
Full Title:	Caleosin-assembled oil bodies as a potential delivery nanocarrier
Article Type:	Original Paper
Section/Category:	Biotechnological products and process engineering
Corresponding Author:	Yun-Peng Chao Feng Chia University Taichung, TAIWAN, REPUBLIC OF CHINA
Corresponding Author Secondary Information:	
Corresponding Author's Institution:	Feng Chia University
Corresponding Author's Secondary Institution:	
First Author:	Chiang Chung-Jen, PhD
First Author Secondary Information:	
All Authors:	Chiang Chung-Jen, PhD Lin Shen-Chuan Lin Li-Jen Chih-Jung Chen Yun-Peng Chao
All Authors Secondary Information:	
Abstract:	Encapsulation of hydrophobic agents with nanocarriers is challenging. Therefore, we have sought to nanoscale artificial oil bodies (NOBs) as an alternative delivery carrier. To constitute NOBs, caleosin (Cal), a structural protein of plant seed oil bodies, was first fused with ZH2 (Cal-ZH2). ZH2 is a bivalent anti-HER2/neu affibody with a high affinity towards the HER2/neu receptor. After overproduction in Escherichia coli, insoluble Cal-ZH2 was isolated and used to assemble NOBs in one step. Consequently, resulting NOBs had a zeta potential around -49 mV and ranged in size from 150 nm to 200 nm. Upon loading with a hydrophobic fluorescence dye, NOBs were found to be selectively internalized into HER2/neu-positive tumor cells. Further analyses showed that more than 90% cells were invaded by dye-loaded NOBs and the cargo dye was released in cells with time. In addition, the in vitro assay revealed the release of the dye from NOBs in a slow and prolong manner. Overall, these results indicate the potential of Cal-based NOBs as a delivery vehicle.
Response to Reviewers:	Dear Professor Steinbuechel: It is my pleasure to submit our revised manuscript (AMAB-D-11-01454) to Appl Microbiol Biotechnol. An itemized list of changes addressing reviewers' comments is as follows. 1. Fig. 5 (C) is changed to Fig. 5 (B). 2. The construction of the fusion protein, Cal fused with ZH2, was described under the Subsection "plasmid construction" in Materials and Methods. See line 14-22, P. 5. 3. As suggested, a scheme illustrating the structure of nanoscale artificial oil bodies (NOBs) was presented in Fig. 8. 4. The advantage of developed NOBs over other delivery systems was described in Discussion. See line 14-26, P. 12. I would love to acknowledge reviewers for their valuable comments. Your kind suggestions on our work are greatly appreciated as well.

Best regards,
Yun-Peng Chao

Professor
Department of Chemical Engineering,
Feng Chia Univeristy

October 25, 2011

Dear Professor Steinbuchel:

It is my pleasure to submit our revised manuscript (AMAB-D-11-01454) to Appl Microbiol Biotechnol. An itemized list of changes addressing reviewers' comments is as follows.

1. Fig. 5 (C) is changed to Fig. 5 (B).
2. The construction of the fusion protein, Cal fused with ZH2, was described under the Subsection "plasmid construction" in Materials and Methods. See line 14-22, P. 5.
3. As suggested, a scheme illustrating the structure of nanoscale artificial oil bodies (NOBs) was presented in Fig. 8.
4. The advantage of developed NOBs over other delivery systems was described in Discussion. See line 14-26, P. 12.

I would love to acknowledge reviewers for their valuable comments. Your kind suggestions on our work are greatly appreciated as well.

Best regards,
Yun-Peng Chao

Professor
Department of Chemical Engineering,
Feng Chia Univeristy

October 25, 2011

Dear Professor Steinbuchel:

It is my pleasure to submit our revised manuscript (AMAB-D-11-01454) to Appl Microbiol Biotechnol. An itemized list of changes addressing reviewers' comments is as follows.

1. Fig. 5 (C) is changed to Fig. 5 (B).
2. The construction of the fusion protein, Cal fused with ZH2, was described under the Subsection "plasmid construction" in Materials and Methods. See line 14-22, P. 5.
3. As suggested, a scheme illustrating the structure of nanoscale artificial oil bodies (NOBs) was presented in Fig. 8.
4. The advantage of developed NOBs over other delivery systems was described in Discussion. See line 14-26, P. 12.

I would love to acknowledge reviewers for their valuable comments. Your kind suggestions on our work are greatly appreciated as well.

Best regards,
Yun-Peng Chao

Professor
Department of Chemical Engineering,
Feng Chia Univeristy

Caleosin-assembled oil bodies as a potential delivery nanocarrier

1
2
3
4
5 Chung-Jen Chiang^{1,*}, Shen-Chuan Lin¹, Li-Jen Lin², Chih-Jung Chen¹, and
6 Yun-Peng Chao^{3,*}
7
8
9

10 ¹ Department of Medical Laboratory Science and Biotechnology, China Medical
11 University, 91 Hsue-Shih Road, Taichung 40402, Taiwan
12
13

14 ² School of Chinese Medicine, China Medical University, Taichung, Taiwan
15
16

17 ³ Department of Chemical Engineering, Feng Chia University, 100 Wen Hwa Road,
18 Taichung 40424, Taiwan
19
20
21
22
23
24
25
26
27
28
29
30
31
32

33
34 * Corresponding authors
35
36

37 Chung-Jen Chiang
38

39 Phone: 886-4-22003366 ext. 7227; FAX: 886-4-22057414.
40
41

42 E-mail address: cjchiang@mail.cmu.edu.tw
43
44
45

46 Yun-Peng Chao
47
48

49 Phone: 886-4-24517250 ext. 3677; FAX: 886-4-24510890
50
51

52 E-mail address: ypchao@fcu.edu.tw
53
54
55
56
57
58
59
60
61
62
63
64
65

1 **Abstract**

2 Encapsulation of hydrophobic agents with nanocarriers is challenging. Therefore, we
3 have sought to nanoscale artificial oil bodies (NOBs) as an alternative delivery
4 carrier. To constitute NOBs, caleosin (Cal), a structural protein of plant seed oil
5 bodies, was first fused with ZH2 (Cal-ZH2). ZH2 is a bivalent anti-HER2/*neu*
6 affibody with a high affinity towards the HER2/*neu* receptor. After overproduction
7 in *Escherichia coli*, insoluble Cal-ZH2 was isolated and used to assemble NOBs in
8 one step. Consequently, resulting NOBs had a zeta potential around -49 mV and
9 ranged in size from 150 nm to 200 nm. Upon loading with a hydrophobic
10 fluorescence dye, NOBs were found to be selectively internalized into
11 HER2/*neu*-positive tumor cells. Further analyses showed that more than 90% cells
12 were invaded by dye-loaded NOBs and the cargo dye was released in cells with time.
13 In addition, the *in vitro* assay revealed the release of the dye from NOBs in a slow
14 and prolong manner. Overall, these results indicate the potential of Cal-based NOBs
15 as a delivery vehicle.

16
17
18
19
20
21
22
23
24
25
26
27
28
29
30
31
32
33
34
35
36
37
38
39
40
41
42
43
44
45
46
47
48
49
50
51
52
53
54
55
56
57
58
59
60
61
62
63
64
65
21 **Keywords:** artificial oil body, Caleosin, targeted delivery, HER2/*neu*

1 **Introduction**

2
3
4
5 3 Plant seeds are rich in oil bodies (OBs) that provide the fuel for seedling growth
6
7 4 (Huang 1996; Napier et al. 1996). OBs consist of a triacylglycerol (TAG) matrix
8
9 5 surrounded by a monolayer of structural protein-bound phospholipids (PLs). Oleosin
10
11 6 (Ole) is recognized as the prominent structural protein associated with OBs (Frandsen
12
13 7 et al. 2001b). This protein has a central hydrophobic region along with two
14
15 8 hydrophilic domains. The former domain is embedded in TAG matrix while the latter
16
17 9 domains protrude outwards. The negative charge of these two terminal domains
18
19 10 provides OBs with the electronegative repulsion that prevents OBs from coalescence.
20
21 11 This in turn results in the stability of OBs in the form of separate entities both *in vivo*
22
23 12 and *in vitro*, and the size of OBs can reach 0.5-2 μm in diameter on average (Tai et al.
24
25 13 2002).

26
27
28 14 OBs can be reconstituted *in vitro* to form artificial oil bodies (AOBs). This is
29
30 15 carried out by subjecting TAG, PLs, and structural proteins to sonication (Tzen et al.
31
32 16 1998; Tzen et al. 1992). Ole is the structural protein that has been primarily employed
33
34 17 for assembling AOBs (Peng et al. 2003). The resulting AOBs are comparable in size,
35
36 18 topology, and stability to those of isolated seed OBs (Tzen and Huang 1992). These
37
38 19 unique structural and topological features of Ole-based AOBs have found many
39
40 20 biotechnological applications, such as the scaffold-assisted refolding and purification
41
42 21 of recombinant proteins (Chiang et al. 2005; Chiang et al. 2007; Peng et al. 2004),
43
44 22 one-step immobilization of enzymes (Chiang et al. 2006), and cargo delivery (Chiang
45
46 23 et al. 2010; Chiang et al. 2011).

47
48
49 24 One promising approach to effectively combat cancers is to employ carriers to
50
51 25 selectively deliver drugs to tumor sites (Farokhzad and Langer 2009). This approach
52
53 26 relies on a drug-loaded carrier conjugated with a bioactive ligand that recognizes the
54
55 27 biomarker of tumor cells. Consequently, a sufficient dose of chemotherapeutic drugs
56
57 28 can reach cancerous loci, thereby minimizing the detrimental side-effect of drugs
58
59 29 toward normal cells (Cho et al. 2008). However, many potent anticancer

1 pharmaceuticals are poorly soluble. Oral or intravenous administration of
2 hydrophobic agents usually leads to low bioavailability of pharmaceuticals due to the
3 aggregate deposition at local sites (Fernandez et al. 2001; Lipinski et al. 2000).
4 Accordingly, various drug carrier systems have been proposed to address this issue,
5 including liposomes (Andresena et al. 2005), synthetic polymers (Zhang et al. 2008),
6 micelles (Torchilin 2005), and others (Cohen and Bernstein 1996). Nevertheless,
7 many technical difficulties need to be overcome before an effective formulation of
8 water-repelling agents is developed (Torchilin 2007).

9 In principle, an effective drug carrier must be small, biocompatible, and
10 biodegradable. AOBs, consisting of natural biomaterials, apparently hold these
11 characteristics. Recently, we have explored the feasibility of AOBs for targeted
12 delivery of hydrophobic agents (Chiang et al. 2010; Chiang et al. 2011). By tailoring
13 the ratio of Ole to oil, nanoscale AOBs (NOBs) could be obtained. Ole was fused with
14 a small bioactive domain, either the arginine-glycine-aspartate (RGD) motif or the
15 bivalent anti-HER2/*neu* affibody (denoted as ZH2). The resulting fusion genes were
16 overexpressed in *Escherichia coli* and the hybrid proteins were isolated for
17 constitution of NOBs. To illustrate, a hydrophobic dye was encapsulated into NOBs
18 that displayed RGD or ZH2 motif on the surface. Upon administration, the RGD- and
19 ZH2-displayed NOBs were selectively internalized into $\alpha_v\beta_3$ integrin- and
20 HER2/*neu*-positive tumor cells, respectively. The internalization efficiency could
21 reach 80% in both cases as revealed by the flow cytometry analysis. Moreover, NOBs
22 entered tumor cells via the endosomal entry pathway and disintegrated with time in
23 response to the low pH condition. The cargo dye was then released into cell cytoplasm.
24 Overall, the results indicate a new application of NOBs in the field of cancer
25 nanotechnology.

26 Caleosin (Cal) is another structural protein associated with seed OBs (Chen et al.
27 1999). The structure of Cal is very similar to that of Ole (Frandsen et al. 2001a). A
28 previous study found that AOBs reconstituted with Cal had a smaller size and
29 exhibited higher stability relative to those with Ole (Liu et al. 2009). Therefore, it was

1 intriguing to examine the feasibility of Cal-based NOBs for targeted delivery of
2 insoluble agents. To this end, Cal was fused with ZH2 (Cal-ZH2). A single domain of
3 ZH2 consists of 58 amino acid residues and exhibits a high binding affinity towards
4 the extracellular domain of HER2/*neu* (Orlova et al. 2006). After overproduction in *E.*
5 *coli*, Cal-ZH2 was isolated and used to assemble NOBs with the size ranging between
6 150 nm and 200 nm. By encapsulation with a hydrophobic dye, Cal-based NOBs were
7 shown to selectively penetrate HER2/*neu*-positive tumor cells in an effective way.
8 Moreover, the cargo dye was released from the pH-responsive nature of Cal-based
9 NOBs upon internalization. The result indicates the potential of Cal-based NOBs as a
10 delivery carrier.

11 **Materials and methods**

12 **Plasmid construction**

13 The ZH2 motif comprises two identical domains of Z_{HER2:342} (Orlova et al. 2006). It
14 was synthesized by Mission Biotech. Co. (Taiwan) and then subcloned into plasmid
15 pBluescriptSKII (Stratagene Co. USA) to obtain plasmid pBlue-ZH2 (Chiang et al.
16 2011). The ZH2 motif was recovered from plasmid pBlue-ZH2 with *EcoRV-HindIII*
17 digestion and incorporated into plasmid pET29a-Cal (Chen et al. 2004) to give
18 plasmid pJO1-Cal-ZH2. This plasmid contains the ZH2 domain fused to the C
19 terminus of Cal and the fusion gene is under the control of the T7 promoter. In
20 contrast, plasmid pET29a-Cal contained Cal alone.

21 **Protein overproduction**

22 *E. coli* strain BL21(DE3) was transformed with plasmid pJO1-Cal-ZH2 and
23 pET29a-Cal. These plasmid-bearing bacterial strains were grown in Luria-Bertani
24 (LB) medium (Miller 1972) at 37°C. To induce protein production, 100 µM Isopropyl
25 β-D-1-thiogalactopyranoside (IPTG) was added to the culture medium. After
26 induction for 4 h, bacteria were harvested by centrifugation and resuspended in 1 mL

1 of 0.01 M sodium phosphate buffer (pH 7.5). Sulfate-polyacrylamide gel
2 electrophoresis (SDS-PAGE) was then conducted to analyze the proteins as previously
3 reported (Chiang et al. 2008).

4 5 Self-assembly of NOBs

6 NOBs were assembled essentially following the previous method (Chiang et al. 2005).
7 In brief, unless stated otherwise the assembly solution (1 mL) consisted of 100 µg
8 olive oil, 150 µg PLs, and 500 µg Cal-ZH2 or Cal in 10 mM sodium phosphate buffer
9 (pH 7.5). The plant oils used here were soybean oil (Taiwan Sugar Co., Taiwan),
10 peanut oil (Leader Price Co., Taiwan), sesame oil (Taisun Co., Taiwan), olive oil
11 (Taisun Co., Taiwan), and mineral oil (Sigma, USA). The solution was then subjected
12 to sonication for 10 s with the amplitude set at 20%. Upon centrifugation, NOBs were
13 removed from the top of the solution. To encapsulate the cargo agent into NOBs, 1 µg
14 yellow GGK dye (Widetex Co., Taiwan) was additionally added to the assembly
15 solution.

16 17 Morphology, size, and stability of NOBs

18 According to the previous report (Chiang et al. 2010), the morphology and size of
19 NOBs were analyzed with a light microscope (Nikon type E600, Japan) and a particle
20 size analyzer (Beckman Coulter, USA), respectively. The stability of NOBs was
21 determined by the turbidity test as reported previously (Chiang et al. 2010). In
22 addition, dye-loaded NOBs were analyzed by Atomic Force Microscopy (AFM) with
23 the NS4/D3100CL/Multi Mode (Digital Instrument, Germany). A drop of the
24 suspension containing NOBs was overlaid onto the mica surface at room temperature.
25 A cantilever was employed to scan the sample with a nominal force constant of 20 N
26 m⁻¹.

27 28 Cell culture

29 Cell cultures were maintained following the reported protocol (Chiang et al. 2011).

1 The human tumor cell lines used here were MDA-MB-231 (ovarian), SKOV3
2 (ovarian), MCF7 (breast), and MCF7/Her18 (HER2-transfected stable cell line). In
3 essence, cell concentration was determined by a hemocytometer. For experiments,
4 cells were seeded into 24-well plates at a cell density of 1×10^5 cells per well.

5
6 Fluorescence microscopy, confocal Microscopy, and flow cytometry

7 Tumor cells were treated with dye-loaded NOBs and then prepared for further
8 analyses as reported previously (Chiang et al. 2011). The anti-HER2/*neu* antibody
9 (Santa Cruz Biotech., USA) was applied to cells. After washing, anti-mouse
10 IgG-TRIAC (Jackson ImmunoResearch Lab., USA) was administrated to stain cell
11 membranes. Meanwhile, cell nuclei were stained with diamidino-2-phenylindole
12 (DAPI) and rinsed with the sodium phosphate buffer. Both fluorescence microscopy
13 (Olympus IX71, Japan) and confocal microscopy (Leica TCS SP2 , Germany) were
14 used to analyze the cells.

15 In addition, tumor cells were seeded to 6-well plate at a cell density of 1×10^5 cells
16 per well. NOBs were then applied to cells for an indicated period of time. Followed
17 by washing, cells were trypsinized and harvested for analyses using a FACScanto
18 flow cytometer system (Becton Dickinson, USA).

19
20 *In vitro* assessment of dye release

21 The release profile of the yellow GGK dye from NOBs was determined following the
22 reported protocol (Chiang et al. 2011). In brief, Cal-ZH2-based NOBs (1 mL) were
23 placed in a dialysis bag (MW cut-off ranging 12,000-14,000 D) that was immersed in
24 the buffer at 37°C with constant stirring. At time intervals, aliquots of the solution
25 (100 μ L) were withdrawn and the content of dye was measured by a
26 spectrofluorometer (FP-6200, Jasco, Japan). The absorbance obtained was normalized
27 to that with the initial content of the dye.

1 Results

3 Self-assembly of NOBs by Cal-ZH2

4 Production of Cal-ZH2 in *E. coli* was analyzed by SDS-PAGE (Fig. 1). Upon
5 induction by IPTG, the bacterial strain was able to overproduce Cal-ZH2 in an
6 insoluble form that was mainly present in the cell lysate (ppt-1). Self-assembly of
7 NOBs was carried out by subjecting the mixture, containing olive oil, PLs, and
8 isolated Cal-ZH2, to sonication. After centrifugation, NOBs sat on the top of mixture
9 solution while no Cal-ZH2 was left in the supernatant fraction (sup-2) and the cell
10 pellet part (ppt-2). NOBs were recovered and heated to liberate incorporated proteins.
11 Consequently, Cal-ZH2 was identified as the main associated protein (NOB). This
12 result indicates the strong association of Cal-ZH2 with oils. Similarly, Cal alone could
13 be overproduced in *E. coli* receiving IPTG induction.

15 Modulation of Cal-ZH2-assembled NOBs

16 According to our previous study (Chiang et al. 2010), NOBs with a smaller size
17 exhibited higher stability. Therefore, three factors affecting the size of NOBs were
18 investigated in a systematic way. NOBs were first assembled with various plant oils at
19 pH 7.5 by fixing the weight ratio of oil to Cla-ZH2 (O/P) at 1:1. As indicated in Fig.
20 2A, NOBs that were prepared from all types of oils except mineral oil exhibited a
21 relatively small and homogenous size. The stability assay for NOBs also showed a
22 similar trend (Fig. 3A).

23 At pH 7.5, NOBs were assembled using olive oil with various O/P ratios. Fig. 2B
24 and 3B show that lower O/P ratios gave a smaller size and higher stability of NOBs.
25 In particular, NOBs had a small and compact morphology when the O/P ratio was
26 lower than 1.

27 Finally, the effect of pH on NOB morphology was examined with the O/P ratio
28 set at 1:1. NOBs tended to have a larger size and lower stability at pH lower than 7
29 (Fig. 2C and 3C). This is in agreement with our previous findings (Chiang et al. 2011).

1 In contrast, NOBs had a smaller size and higher stability at an alkali condition. As
2 further analyzed, NOBs assumed a spherical shape with the size ranging 150-200 nm
3 by AFM (Fig. 4), and their zeta potential was estimated to be -49.1 ± 2.3 mV.

4 5 Selective internalization of Cal-ZH2-assembled NOBs

6 The functionality of ZH2 displayed on Cal-based NOBs was further investigated. To
7 clearly illustrate, a hydrophobic fluorescence dye was encapsulated into NOBs with or
8 without ZH2. Upon administration of the fluorescent dye-loaded NOBs, strong
9 fluorescent signals could be detected in HER2/*neu*-positive cells (e.g., MCF7/Her18
10 and SKOV3) and the signal intensity increased in a NOB dose-dependent manner (Fig.
11 5A). In contrast, the signal was absent for HER2/*neu*-negative cells (e.g., MCF7 and
12 MDA-MB-231). Similarly, no fluorescence could be observed in any type of tumor
13 cells that were exposed to NOBs free of ZH2 (data not shown). Overall, the results
14 suggest the functional display of ZH2 via Cal onto the surface of NOBs. This in turn
15 leads to the specific association of functionalized NOBs with HER2/*neu*-positive
16 cells.

17 In addition, the localization of internalized NOBs was confirmed by confocal
18 microscopy. Fig. 5B shows that the fluorescent dye-loaded NOBs were located in the
19 cytoplasm of HER2/*neu*-positive cells. It clearly indicates the ability of functionalized
20 NOBs to target and penetrate HER2/*neu*-positive cells.

21 22 Internalization efficiency of Cal-ZH2-assembled NOBs

23 The internalization efficiency of Cal-ZH2-assembled NOBs was calculated as the
24 percentage of fluorescence-emitting cells in the whole cell population. After
25 administration of fluorescence dye-loaded NOBs for various time periods, tumor cells
26 were processed for analyses by flow cytometry. As depicted in Fig. 6A, internalization
27 efficiency of ZH2-displayed NOBs towards HER2/*neu*-positive cells generally
28 increased with the longer administration time. The maximum internalization
29 efficiency was more than 90% for SKOV3 and MCF7/Her18 cells upon

1 administration of functionalized NOBs for 60 and 120 min, respectively. A similar
2 observation could also be obtained with fluorescence microscopy (Fig. 6B).

3 4 Release of the cargo dye

5 As reported recently, Ole-based NOBs displaying ZH2 were internalized into tumor
6 cells via the endosomal entry pathway (Chiang et al. 2011). The cargo dye was
7 released as a result of the instability of Ole-based NOBs at an acidic condition.
8 Therefore, it promoted us to investigate the control-and-release feature of NOBs
9 assembled by Cal-ZH2. SKOV3 cells were then administrated with fluorescent
10 dye-loaded NOBs (25 $\mu\text{g}/\text{mL}$) for 1 h. After washing, the fluorescent signals within
11 cells were monitored by confocal microscopy along the time course. As shown in Fig.
12 7A, the signals in the cells faded with time. After 5 days, the fluorescent images in the
13 cells were barely detectable. The result implies that the cargo dye is released from
14 Cal-based NOBs and gradually decays within the cells.

15 Furthermore, the dialysis analysis was conducted to analyze the *in vitro* release
16 profiles of the cargo dye from Cal-ZH2-assembled NOBs. Fig. 7B shows that an
17 initial burst release occurred at the first 6 h. The released cargo dye reached 55% at
18 pH 6.5 and 40% at pH7.5. After that, the dye was released in a stable and slow way.
19 This sustained and prolonged release curve resembles the typical profile as commonly
20 reported for many drug delivery systems (Kim et al. 2007; Yang et al. 2002).

21 22 **Discussion**

23
24 Nanotechnology has transformed the medication method for treatment of diseases.
25 Apparently, targeted therapy is an emerging technology that receives the most
26 intensive study. In essence, the approach relies on a nanocarrier that delivers
27 therapeutic agents to target cells. However, one pressing challenge is to overcome the
28 technical difficulties in the robust formulation of hydrophobic drugs with nanocarriers.
29 In this study, we have sought to Cal-based NOBs as an alternative nanocarrier.

1 Self-assembled NOBs comprise a central oil core that is enveloped by a monolayer of
2 Cal-bound lipid (Fig. 8). To make NOBs functional, the anti-HER2/*neu* motif (e.g.,
3 ZH2) was displayed at their surface by linkage to the C-terminus of Cal. It is known
4 that HER2/*neu* belongs to the human epidermal growth factor receptor family (Hung
5 and Lau 1999). An abnormal and uncontrolled expression of HER2/*neu* can
6 eventually lead to the progression of many aggressive tumors (Citri and Yarden 2006).
7 As illustrated, Cal-based NOBs with surface display of ZH2 could specifically
8 penetrate HER2/*neu*-positive tumor cells (Fig. 5A and 5B). This indicates that fusion
9 of Cal with the bioactive motif provides a simple and feasible way for
10 functionalization of NOBs.

11 The translocation path of the HER2/*neu* receptor into cells was proposed
12 previously (Giri et al. 2005). The receptor enters cells by the endocytic internalization
13 and then interacts with importin, a transport protein. Escorted by the nuclear pore
14 protein, HER2/*neu* travels to cell nucleus. In agreement with this proposed pathway,
15 ZH2 on the surface of NOBs interacted with HER2/*neu* of tumor cells, leading to the
16 internalization of NOBs into cell endosomes (Chiang et al. 2011). This translocation
17 mechanism also resulted in the heterogeneous distribution of internalized NOBs in
18 cells (Fig. 5B). Moreover, the internalization behavior of Cal-based NOBs was
19 time-dependent (Fig. 6B), which is consistent with the invasion kinetics of
20 anti-HER2/*neu* affibody-conjugated materials as reported (Alexis et al. 2008). At the
21 acidic condition in cell endosomes (Ohkuma and Poole 1978; Yamashiro et al. 1983),
22 NOBs started to disintegrate with the release of the cargo dye (Fig. 7A). Based on the
23 *in vitro assay*, the release rate of cargo dyes from Cal-based NOBs is slower than that
24 from Ole-based NOBs (Fig. 7B). After 7 h at pH 6.5, there was 55% cargo dyes being
25 liberated for Cal-based NOBs whereas more than 90% was released for Ole-based
26 NOBs (Chiang et al. 2011). The result implies the potential of Cal-based NOBs for the
27 long-acting release system.

28 The size of Cal-based NOBs was tunable. As indicated in Fig. 2, the type of plant
29 oils could affect the morphology of NOBs. This result suggests that Cal-ZH2 likely

1 interacts differentially with various TAG compositions of oils. More Cal-ZH2 than oil
2 in the formulation could result in smaller and more stable NOBs. It indicates that
3 more terminal domains (bearing a negative charge) of Cal could contribute stronger
4 repulsion force to maintain the integrity of NOBs. However, under an acidic condition,
5 the electronegative repulsion force is likely negated as a result of neutralization by H⁺,
6 which leads to coalescence of NOBs. The size of NOBs assembled by Cal can be
7 tailored to reach less than 200 nm and is smaller than that with Ole (Chiang et al.
8 2011). In particular, the zeta potential of Cal-based NOBs (< -30 mV) was very high,
9 suggesting that they are stable (Lee et al. 2007). Moreover, Cal-based NOBs is
10 superior to Ole-based counterparts in terms of internalization efficiency (e.g., the
11 percentage of fluorescence-emitting cells and incubation time) (Chiang et al. 2011).
12 Regardless of the cell type, the uptake efficiency of Cal-based NOBs could reach
13 above 90% with incubation time less than 2 h (Fig. 6A).

14 As well recognized, liposomes and polymeric micelles are two primary
15 nanocarriers developed for a wide range of applications (Elbayoumi et al. 2007;
16 Shmeedaa et al. 2009; Sugarman et al. 1996). Liposomes have a lipid-enclosed
17 aqueous space that is not applicable for entrapment of water-repelling agents.
18 Polymeric micells contain a hydrophobic center surrounded by a hydrophilic shell
19 and are effective for encapsulation of hydrophobic cargos. However, both carriers
20 need to be conjugated with a functional ligand by a chemical modification before
21 they can selectively target tumor cells. In contrast, NOBs are oil droplets that
22 facilitate the entrapment of hydrophobic agents. They are biocompatible and can be
23 self-assembled in an easy and reproducible way. Simply fusing a bioactive motif
24 with Cal can result in functional NOBs that are highly invasive and featured with an
25 acid-triggered release nature. In conclusion, the advance of this novel approach may
26 open a new avenue in the filed of cancer nanotechnology.

27 28 **Acknowledgement**

29 We like to acknowledge Instrument Center of R&D Office at China Medical

1 University for technical assistance. This work was supported by National Science
2 Council of Taiwan (NSC 99-2313-B-039-003-MY3, NSC
3 98-2221-E-035-029-MY3), China Medical University (CMU100-S-29), and
4 Ministry of Economic Affairs (99-EC-17-A-10-S1-156).

6 **References**

- 8 Alexis F, Basto P, Levy-Nissenbaum E, Radovic-Moreno F, Zhang L, Pridgen E,
9 Wang AZ, Marein SL, Westerhof K, Molnar LK and others (2008)
10 HER-2-targeted nanoparticle-affibody bioconjugates for cancer therapy.
11 ChemMedChem 3:1839-1843.
- 12 Andresena TL, Jensenb SS, Jørgensen K (2005) Advanced strategies in liposomal
13 cancer therapy: problems and prospects of active and tumor specific drug
14 release. Prog Lipid Res 44:68-97.
- 15 Chen JC, Tsai CC, Tzen JTC (1999) Cloning and secondary structure analysis of
16 caleosin, a unique calcium-binding protein in oil bodies of plant seeds. Plant
17 Cell Physiol 40:1079-1086.
- 18 Chen MC, Chyan CL, Lee TT, Huang SH, Tzen JTC (2004) Constitution of stable
19 artificial oil bodies with triacylglycerol, phospholipid, and caleosin. J Agri
20 Food Chem 52:3982-3987.
- 21 Chiang CJ, Chen CJ, Chang CH, Chao YP (2010) Selective delivery of cargo entities
22 to tumor cells by nanoscale artificial oil bodies. J Agri Food Chem
23 58:11695-11702.
- 24 Chiang CJ, Chen HC, Chao YP, Tzen JTC (2005) Efficient system of artificial oil
25 bodies for functional expression and purification of recombinant nattokinase
26 in *Escherichia coli*. J Agric Food Chem 53:4799-4804.
- 27 Chiang CJ, Chen HC, Chao YP, Tzen JTC (2007) One-step purification of insoluble
28 hydantoinase overproduced in *Escherichia coli*. Protein Expr Purif 52:14-18.
- 29 Chiang CJ, Chen HC, Kuo HF, Chao YP, Tzen JTC (2006) A simple and effective
30 method to prepare immobilized enzymes using artificial oil bodies. Enzyme
31 Microb Technol 39:1152-1158.
- 32 Chiang CJ, Chern JT, Wang JY, Chao YP (2008) Facile immobilization of evolved
33 *Agrobacterium radiobacter* carbamoylase with high thermal and oxidative
34 stability. J Agri Food Chem 56:6348-6354.
- 35 Chiang CJ, Lin LJ, Lin CC, Chang CH, Chao YP (2011) Selective internalization of

1 self-assembled artificial oil bodies by HER2/neu-positive cells. *Nanotechnol*
2 22:015102.

3 Cho K, Wang X, Nie S, Chen Z, Shin DM (2008) Therapeutic nanoparticles for drug
4 delivery in cancer. *Clin Cancer Res* 14:1310-1316.

5 Citri A, Yarden Y (2006) EGF-ERBB signalling: towards the systems level. *Nat Rev*
6 *Mol Cell Biol* 7:505-516.

7 Cohen SN, Bernstein H (1996) Microparticulate systems for the delivery of proteins
8 and vaccines. New York: Marcel Dekker.

9 Elbayoumi TA, Pabba S, Roby A, Torchilin VP (2007) Antinucleosome
10 antibody-modified liposomes and lipid-core micelles for tumor-targeted
11 delivery of therapeutic and diagnostic agents. *J Liposome Res* 17:1-14.

12 Farokhzad OC, Langer R (2009) Impact of nanotechnology on drug delivery. *ACS*
13 *Nano* 3:16-20.

14 Fernandez AM, Van derpoorten K, Dasnois L, Lebtahi K, Dubois V, Lobl TJ,
15 Gangwar S, Oliyai C, Lewis ER, Shochat D and others (2001)
16 N-Succinyl-(β -alanyl-L-leucyl-L-alanyl-L-leucyl)doxorubicin: an
17 extracellularly tumor-activated prodrug devoid of intravenous acute toxicity.
18 *J Med Chem* 44:3750-3753.

19 Frandsen GI, Mundy J, Tzen JTC (2001a) Oil bodies and their associated proteins,
20 oleosin and caleosin. *Physiol Plant* 112:301-307.

21 Frandsen GI, Mundy J, Tzen JTC (2001b) Oil bodies and their associated proteins,
22 oleosin and caleosin. *Physiol Plant* 112:301-307.

23 Giri DK, Ali-Seyed M, Li LY, Lee DF, Ling P, Bartholomeusz G, Wang SC, Hung
24 MC (2005) Endosomal transport of ErbB-2: mechanism for nuclear entry of
25 the cell surface receptor. *Mol Cell Biol* 25:11005-11018.

26 Huang AH (1996) Oleosins and oil bodies in seeds and other organs. *Plant Physiol*
27 110:1055-1061.

28 Hung MC, Lau YK (1999) Basic science of HER2/*neu*: a review. *Semin Oncol*
29 26:51-59.

30 Kim GY, Tyler BM, Tupper MM, Karp JM, Langer RS, Brem H, Cima MJ (2007)
31 Resorbable polymer microchips releasing BCNU inhibit tumor growth in the
32 rat 9L flank model. *J Control Release* 123:172-178.

33 Lee HK, Lee HY, Jeon JM (2007) Codeposition of micro- and nano-sized SiC
34 particles in the nickel matrix composite coatings obtained by electroplating.
35 *Surf Coat Tech* 201:4711-4717.

36 Lipinski CA, Lombardo F., Dominy BW, Feeney PJ (2000) Experimental and
37 computational approaches to estimate solubility and permeability in drug
38 discovery and development settings. *Adv Drug Deliv Rev* 46:3-36.

- 1 Liu TH, Chyan CL, Li FY, Tzen JTC (2009) Stability of artificial oil bodies
2 constituted with recombinant caleosins. *J Agri Food Chem* 57:2308-2313.
- 3 Miller JH (1972) Experiments in molecular genetics. Cold Spring Harbor, New York:
4 Cold Spring Harbor Laboratory.
- 5 Napier JA, Stobart AK, Shewry PR (1996) The structure and biogenesis of plant oil
6 bodies: the role of the ER membrane and the oleosin class of proteins. *Plant*
7 *Mol Biol* 31:945-956.
- 8 Ohkuma S, Poole B (1978) Fluorescence probe measurement of the intralysosomal
9 pH in living cells and the perturbation of pH by various agents. *Proc Natl*
10 *Acad Sci U S A* 75:3327-3331.
- 11 Orlova A, Magnusson M, Eriksson TLJ, Nilsson M, Larsson B, Hoiden-Guthenberg
12 I, Widstrom C, Carlsson J, Tolmachev V, Stahl S and others (2006) Tumor
13 imaging using a picomolar affinity HER2 binding affibody molecule. *Cancer*
14 *Res* 66:4339-4348.
- 15 Peng CC, Chen JCF, Shyu DJH, Chen MJ, Tzen JTC (2004) A system for
16 purification of recombinant proteins in *Escherichia coli* via artificial oil
17 bodies constituted with their oleosin-fused polypeptides. *J Biotechnol*
18 111:51-57.
- 19 Peng CC, Lin IP, Lin CK, Tzen JTC (2003) Size and stability of reconstituted
20 sesame oil bodies. *Biotechnol Prog* 19:1623-1626.
- 21 Shmeedaa H, Tzemacha D, Maka L, Gabizon A (2009) Her2-targeted pegylated
22 liposomal doxorubicin: retention of target-specific binding and cytotoxicity
23 after *in vivo* passage. *J Control Release* 136:155-160.
- 24 Sugarman SM, Zou YY, Wasan K, Poirot K, Kumi R, Reddy S, Perez-Soler R (1996)
25 Lipid-complexed camptothecin: formulation and initial biodistribution and
26 antitumor activity studies. *Cancer Chemother Pharmacol* 37:531-538.
- 27 Tai SSK, Chen MCM, Peng CC, Tzen JTC (2002) Gene family of oleosin isoforms
28 in sesame seed oil bodies. *Biosci Biotechnol Biochem* 66:2146-2153.
- 29 Torchilin VP (2005) Lipid-core micelles for targeted drug delivery. *Curr Drug*
30 *Delivery* 2:319-327.
- 31 Torchilin VP (2007) Micellar nanocarrier: pharmaceutical perspectives. *Pharma Res*
32 24:1-16.
- 33 Tzen JTC, Chuang RL, Chen JC, Wu LS (1998) Coexistence of both oleosin
34 isoforms on the surface of seed oil bodies and their individual stabilization to
35 the organelles. *J Biochem* 123: 318-323.
- 36 Tzen JTC, Huang AH (1992) Surface structure and properties of plant seed oil
37 bodies. *J Cell Biol* 117:327-335.
- 38 Tzen JTC, Lie GC, Huang AH (1992) Characterization of the charged components

1 and their topology on the surface of plant seed oil bodies. J Biol Chem
2 267:15626-15634.

3 Yamashiro DJ, Fluss SR, Maxfield FR (1983) Acidification of endocytic vesicles by
4 an ATP-dependent proton pump. J Cell Biol 97:929-934.

5 Yang Z, Zhang Y, Markland P, Yang VC (2002) Poly(glutamic acid) poly(ethylene
6 glycol) hydrogels prepared by photoinduced polymerization: synthesis,
7 characterization, and preliminary release studies of protein drugs. J Biomed
8 Mater Res 62:14-21.

9 Zhang L, Chan JM, Gu FX, Rhee JW, Wang AZ, Radovic-Moreno AF, Alexis F,

10 Langer R, Farokhzad OC (2008) Self-assembled lipid- polymer hybrid

11 nanoparticles: a robust drug delivery platform. ACS Nano 2:1696-1702.

1 **Figure legends:**
2
3

4 **Figure 1.** SDS-PAGE analyses of Cal-ZH2 production in *E. coli*. *E. coli* strain bearing
5 plasmid pJO1-Cal-ZH2 (left panel) or pET29a-Cal (right panel) was cultured and
6 induced (+IPTG) for protein production. By centrifugation, proteins of plasmid
7 pJO1-Cal-ZH2-bearing bacteria were fractioned into the soluble part (sup-1) and
8 insoluble part (ppt-1). Insoluble Cal-ZH2 was used for assembly of NOBs with two
9 fractions left after centrifugation, including the supernatant (sup-2) and precipitate
10 (ppt-2). NOBs were recovered from the top of the solution and heated to release the
11 protein (AOB).
12
13
14
15
16
17
18
19
20
21
22
23
24

25 **Figure 2.** Morphology of Cal-based NOBs at various conditions. Morphology of
26 Cal-based NOBs was analyzed by light microscopy. (A) Assembly of Cal-based NOBs
27 with various plant oils, including (1) mineral oil, (2) peanut oil, (3) soybean oil, (4)
28 olive oil, and (5) sesame oil. (B) Assembly of Cal-based NOBs with various O/P
29 ratios at (1) 10:1, (2) 2:1, (3) 1:1, (4) 1:5, and (5) 1:10. (C) Assembly of Cal-based
30 NOBs at pH (1) 6.5, (2) 7.0, (3) 7.5, (4) 8.0, and (5) 9.0. The scale bar equals 2 μm .
31
32
33
34
35
36
37
38
39

40 **Figure 3.** Stability of Cal-based NOBs at various conditions. The stability of NOBs
41 was determined by the turbidity test as described. (a) The stability profile of NOBs
42 assembled with various types of oils. (b) The stability profile of NOBs assembled at
43 various O/P ratios. (c) The stability profile of NOBs assembled at various pHs.
44
45
46
47
48
49

50 **Figure 4.** Morphology of NOBs by AFM. NOBs were assembled with the O/P ratio at
51 1:5 and at pH 7.5.
52
53
54
55

56 **Figure 5.** Selective internalization of NOBs. NOBs were assembled with Cal-ZH2 and
57 encapsulated with 1 $\mu\text{g}/\text{mL}$ yellow GGK dye. The resulting NOBs (green) were added
58
59
60
61
62
63
64
65

1 to 1×10^5 cells to reach the indicated concentration (shown on the left) and incubated
2 for 2 h. After repeated washing for 3 times, cells were processed for further analyses.
3
4 (A) Analysis by fluorescence microscopy. Cell nuclei (blue) and the HER2/*neu*
5 receptor (red) were stained with DAPI and anti-HER2/*neu* antibody, respectively.
6
7 Individual images were taken and then merged as shown on the right. (B) Analysis by
8
9 confocal laser scanning microscopy (CLSM). After treated with Cal-ZH2-based
10 NOBs, SKOV3 cells were analyzed by CLSM. The insets show the two
11 three-dimensional reconstruction sections, including X-Z (bottom) and Y-Z (right)
12 sections.
13
14
15
16
17
18
19
20
21

22 Figure 6. Internalization efficiency of NOBs by flow cytometry and confocal
23 microscopy. Refer to Fig. 5, cells were treated with Cal-based NOBs (green) at 25
24 $\mu\text{g}/\text{mL}$. (A) Analysis by flow cytometry. Various cells were exposed to ZH2-displayed
25 (Cal-ZH2) or ZH2-lacking NOBs (Cal) for an indicated time. All experiments were
26 conducted in triplicate. (B) Analysis by fluorescence microscopy. Incubation time was
27 shown on the left of each panel.
28
29
30
31
32
33
34
35

36 Figure 7. Release of the fluorescence dye carried by NOBs. (A) Analysis by confocal
37 microscopy. SKOV3 cells were treated with Cal-ZH2-based NOBs that carried the
38 hydrophobic dye. The fluorescence emitted by internalized NOBs in the cells was
39 analyzed by confocal microscopy on (1) day 0, (2) day 1, (3) day 3, and (4) day 5. (B)
40 *In vitro* dye release profile. NOBs were loaded with the dye ($6.25 \mu\text{g}/\text{mL}$) and
41 assessed for the dye release at pH 6.5 (●) or pH 7.5 (○) for 24 h. The experiment was
42 conducted in triplicate.
43
44
45
46
47
48
49
50
51
52
53
54
55

56 Figure 8. A scheme illustrating the structure of Cal-ZH2-based NOBs. For clear
57 illustration, a slice section of NOBs was removed to uncover the internal structure.
58
59
60
61
62
63
64
65

1 Like plant OBs, NOBs are mainly composed of a TAG matrix enclosed by a
2
3 monolayer of Cal-bound PLs. The ZH2 motif linked to Cal is displayed at the surface
4
5 of NOBs, consequently leading NOBs to targeting HER2/*neu*-expressing tumor cells.
6
7
8
9
10
11
12
13
14
15
16
17
18
19
20
21
22
23
24
25
26
27
28
29
30
31
32
33
34
35
36
37
38
39
40
41
42
43
44
45
46
47
48
49
50
51
52
53
54
55
56
57
58
59
60
61
62
63
64
65

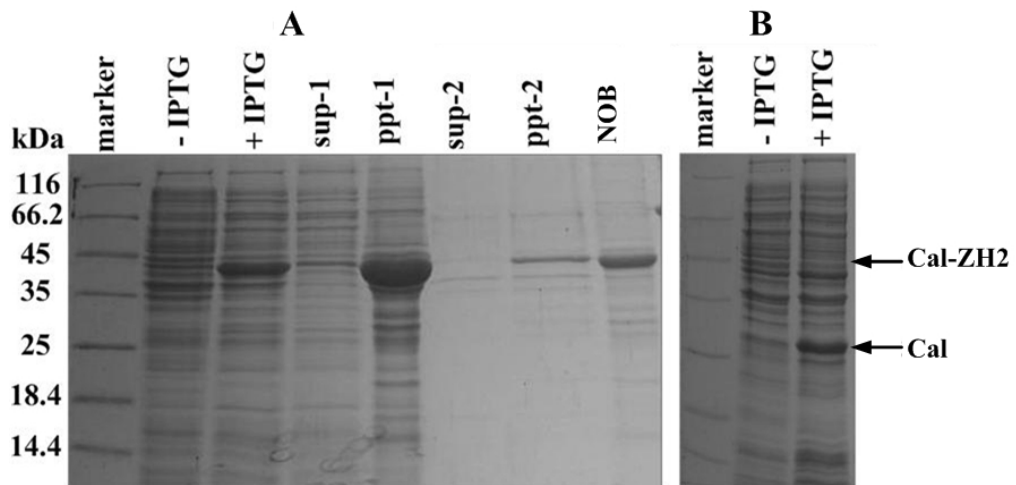


Figure 1

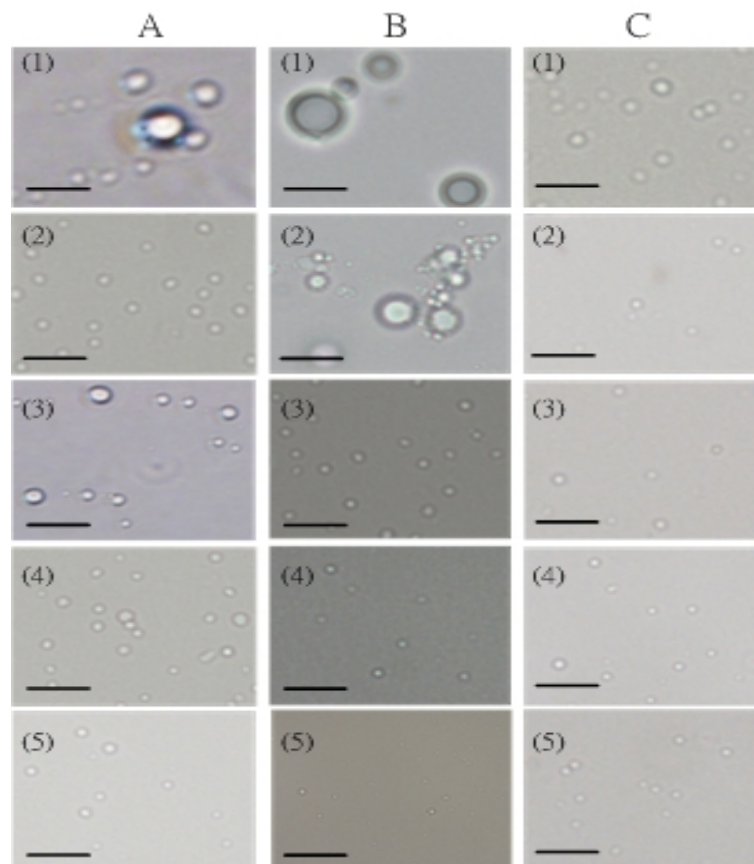


Figure. 2

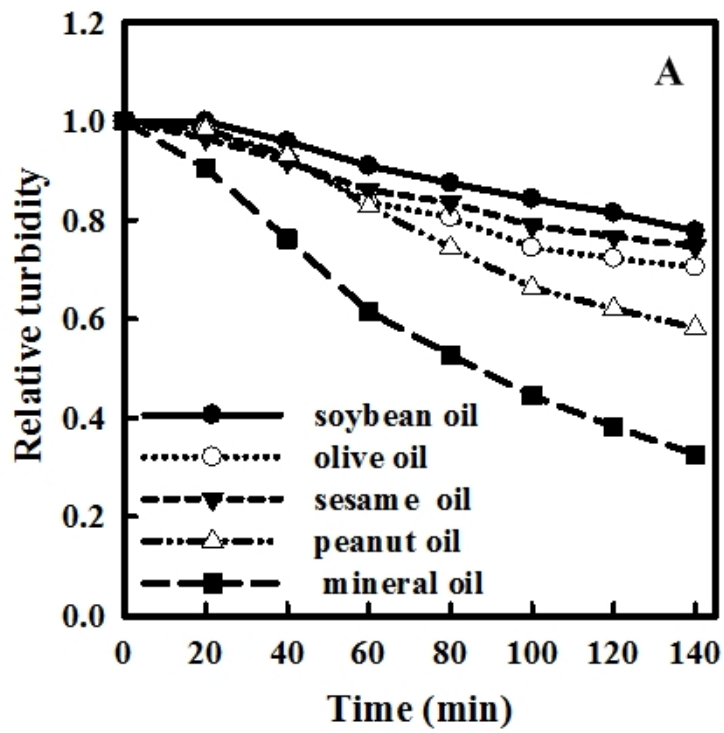


Figure 3A

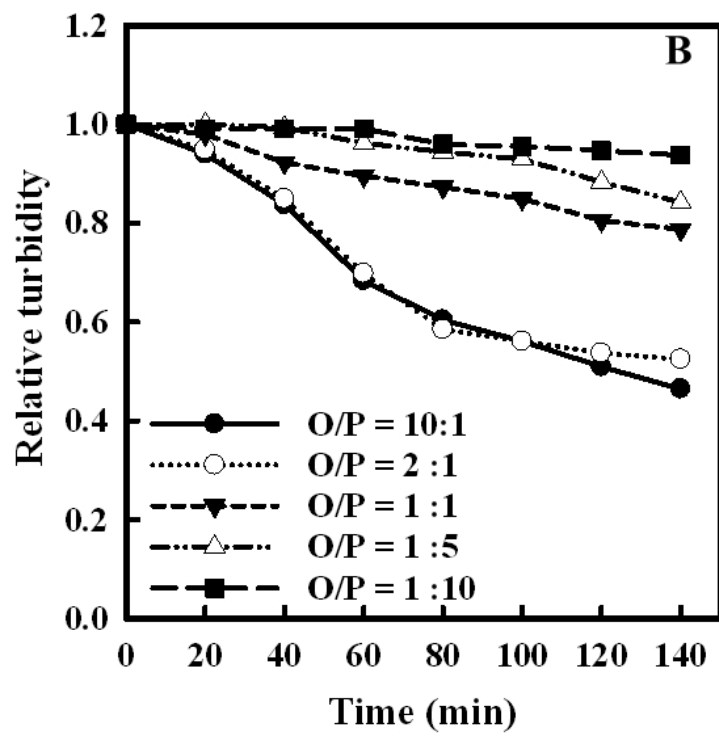


Figure 3B

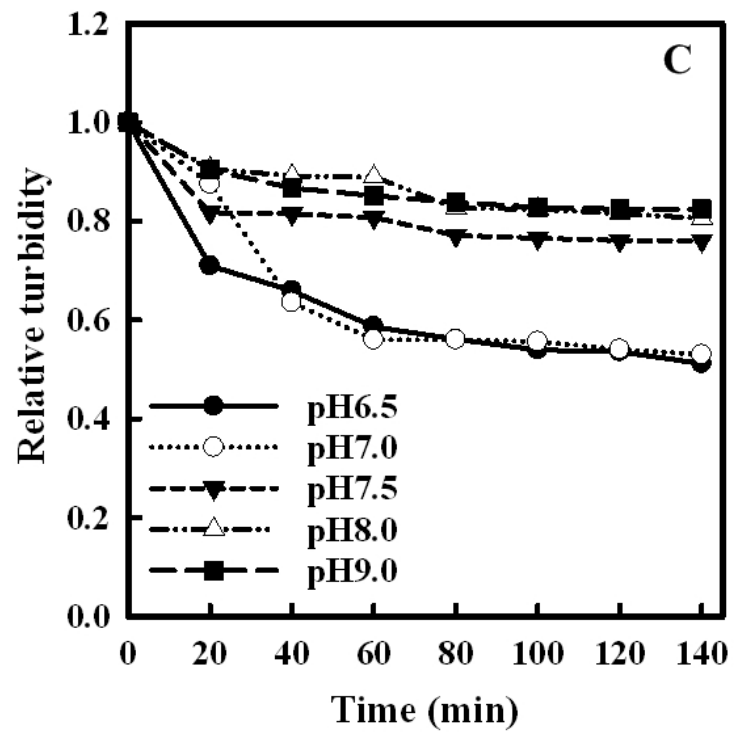


Figure 3C

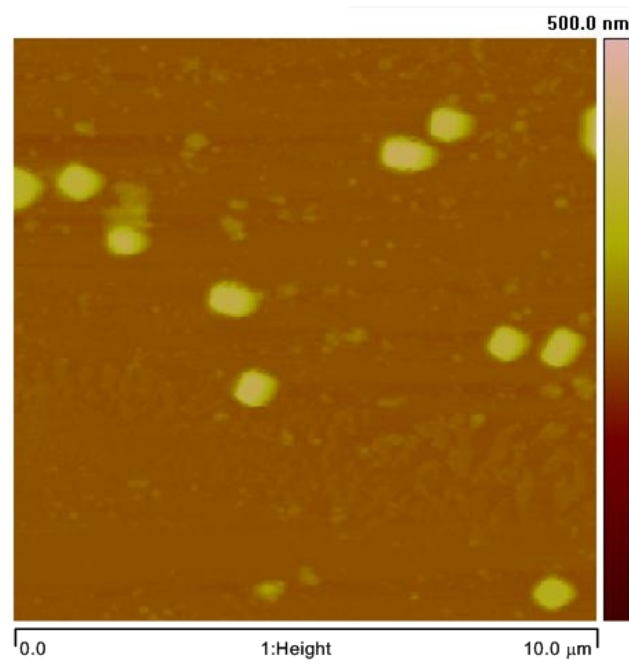


Figure 4

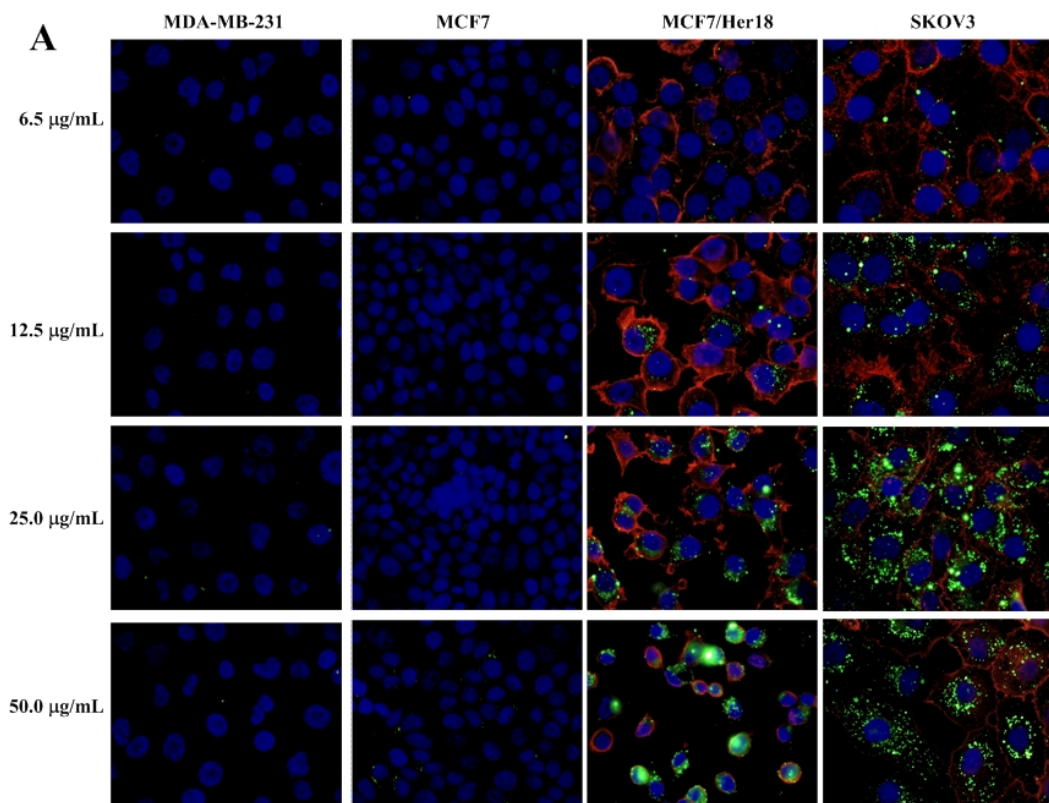


Figure 5A

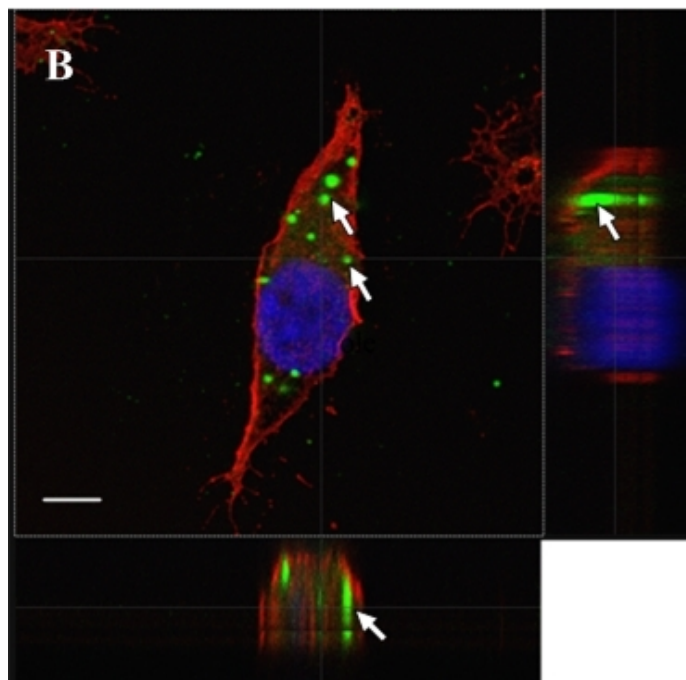


Figure 5B

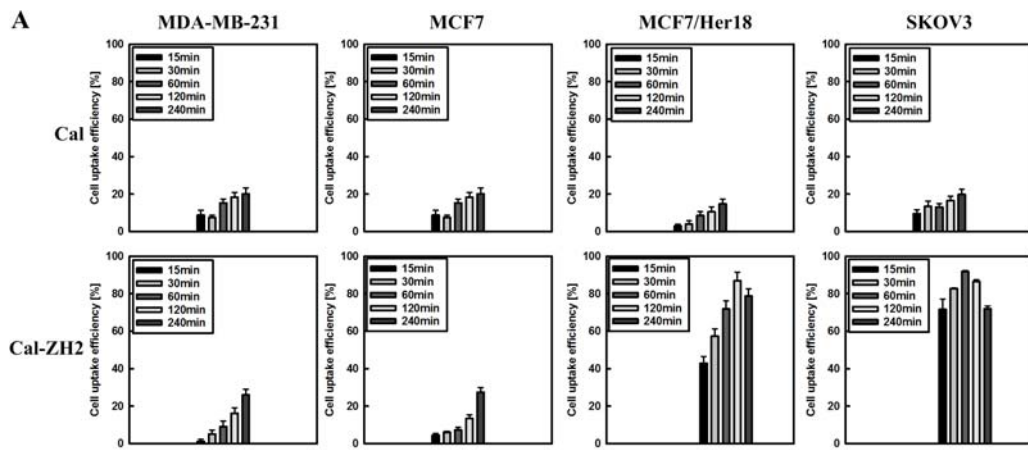


Figure 6A

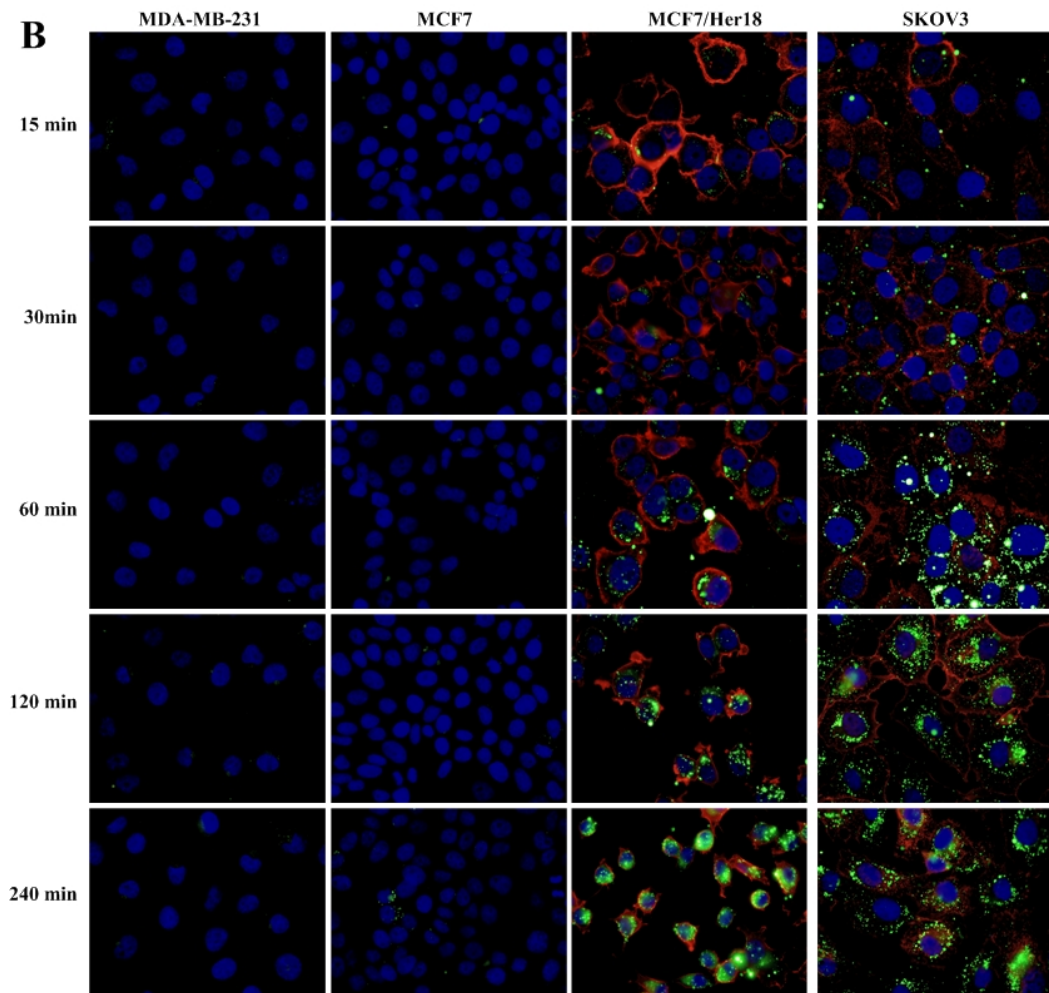


Figure 6B.

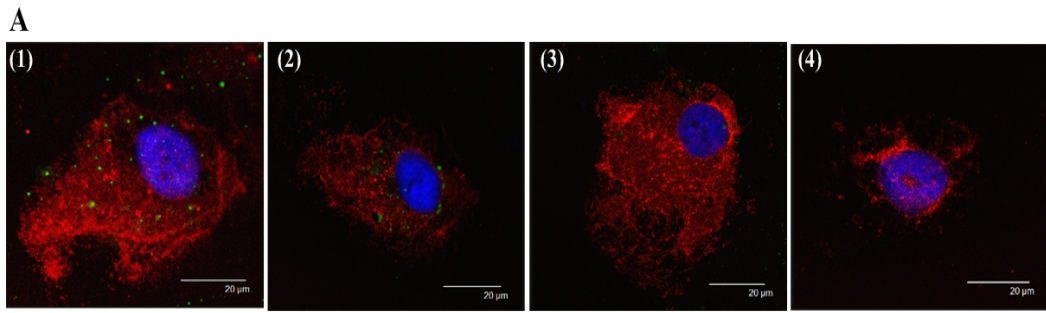


Figure 7A.

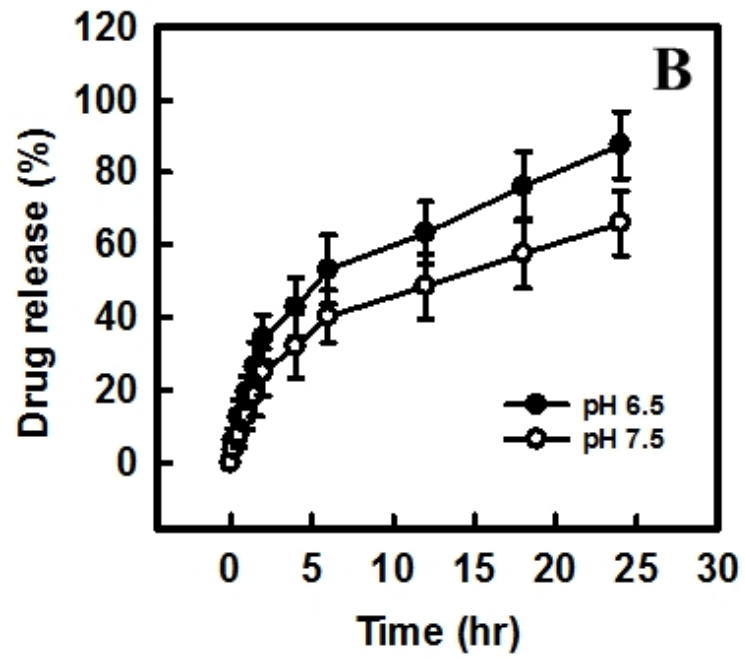


Figure 7B.

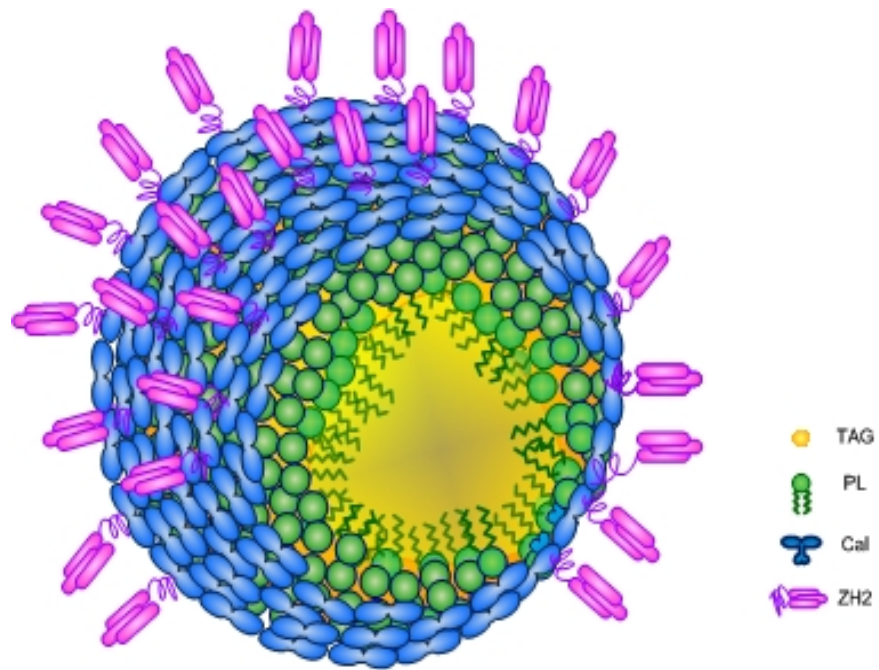


Figure 8.